Food and Chemical Toxicology 111 (2018) 546–556

Contents lists available at ScienceDirect

Food and Chemical Toxicology

journal homepage: www.elsevier.com/locate/foodchemtox

Stable PEG-coated silver nanoparticles – A comprehensive toxicological profile

Iulia Pinzaru[a,1], Dorina Coricovac[a,1], Cristina Dehelean[a,*], Elena-Alina Moacă[a], Marius Mioc[a], Flavia Baderca[b], Ioana Sizemore[c], Seth Brittle[c], Daniela Marti[d], Cornelia Daniela Calina[e], Aristidis M. Tsatsakis[f], Codruţa Şoica[a]

[a] Faculty of Pharmacy, "Victor Babes" University of Medicine and Pharmacy, 2nd Eftimie Murgu Sq., Timisoara, 300041, Romania
[b] Faculty of Medicine, "Victor Babes" University of Medicine and Pharmacy, 2nd Eftimie Murgu Sq., Timisoara, 300041, Romania
[c] Department of Chemistry, Wright State University, Dayton, OH, 45435-0001, USA
[d] Western University Vasile Goldis Arad, 94 Revolutiei Blvd., 310025, Arad, Romania
[e] Faculty of Pharmacy, University of Medicine and Pharmacy Craiova, Petru Rares 2, 200349, Craiova, Romania
[f] Department of Forensic Sciences and Toxicology, Faculty of Medicine, University of Crete, Heraklion 71003, Greece

ARTICLE INFO

Keywords:
Silver nanoparticles
Acute/subacute toxicity
In vitro
SKH-1 mice
Non-invasive techniques
Mast cells

ABSTRACT

The present study was purported to assess the toxicological profile of bare and polyethylene glycol (PEG) coated spherical silver nanoparticles (AgNPs) by means of *in vitro* (on human keratinocytes – HaCat cells) and *in vivo* non-invasive tests (after intraperitoneal - i.p. administration to mice). Bare and PEG-coated AgNPs were synthesized by applying Turkevich's method slightly modified. The physico-chemical characterization revealed the formation of stable, spherical AgNPs and PEG-AgNPs, with narrow size distributions and mean hydrodynamic sizes in the range of 19 nm and 50 nm, respectively.

Toxicity data revealed a dose-dependent safe profile for low concentrations of test compounds (< 10 μM) in terms of cell viability, whereas higher concentrations were associated with a high rate of cell mortality. *In vivo* acute/subacute toxicity data showed no denotive changes in mice health status after i.p. administration. Histological observations of internal organs and the biochemical parameters analyzed together with the other biological observations showed a low toxicity level with no major differences related to control, albeit at skin level a reduced number of mast cells was detected. All these observations provide strong support for the idea that coated silver nanoparticles could be applied as targeted nanocarriers for skin pathologies and diagnostic.

1. Introduction

Nanotechnology may offer an effective alternative to conventional chemotherapy through several advantages provided by drug-nano-carriers: high drug load, increased half-life, targeted delivery, and lower toxicity (Banerjee and Sengupta, 2011). Nanoparticles were used extensively in recent years in a myriad of domains including: aerospace engineering, consumer products (food packages), nano-electronics, environmental safety and medical healthcare (Ahamed et al., 2010). The nanoparticles were described as structures or systems that possess at least one dimension smaller than 100 nm in length; the origin of the term "nano" is Greek and it means "dwarf" (Ahamed et al., 2010; Arora et al., 2012). Metal nanoparticles have acceded into the biomedical area due to their ability to act as both diagnostic and drug delivery agents, thus qualifying as theranostic compounds (Conde et al., 2012).

The biologic effects of silver, as antibacterial and antimicrobial agent, are well-known and were considered winning features in the selection of AgNPs for the use in biomedicine (Chaloupka et al., 2010). The antibacterial and antimicrobial properties recommend silver nanoparticles as efficient agents in food technology field in terms of food safety, quality and augmented shelf life (Mohanta et al., 2017).

Besides the antibacterial activity of the silver, there were described other biological effects, like anti-inflammatory, regenerative and role in cauterization, and the correspondent effects of the AgNPs were: prophylactic environmental effect (in paints and disinfectants), prophylactic antibacterial effect (as coating surfaces for venous catheters and

* Corresponding author.
E-mail addresses: iuliapinzaru@umft.ro (I. Pinzaru), dorinacoricovac@umft.ro (D. Coricovac), cadehelean@umft.ro (C. Dehelean), alina.moaca@umft.ro (E.-A. Moacă), marius.mioc@umft.ro (M. Mioc), flaviabaderca@gmail.com (F. Baderca), ioana.pavel@wright.edu (I. Sizemore), brittle.3@wright.edu (S. Brittle), dana_m73@yahoo.com (D. Marti), calinadaniela@gmail.com (C.D. Calina), tsatsaka@uoc.gr (A.M. Tsatsakis), codrutasoica@umft.ro (C. Şoica).
[1] Authors that contributed equally.

https://doi.org/10.1016/j.fct.2017.11.051
Received 9 October 2017; Received in revised form 24 November 2017; Accepted 25 November 2017
Available online 02 December 2017

neurosurgical shunts, in bone cement and vascular implants) and protection against infection (wound dressings) (Chaloupka et al., 2010). Furthermore, AgNPs were demonstrated to have anticancer effects, being capable to generate DNA damage, cell cycle arrest, oxidative stress, apoptosis and necrosis (Muhammad et al., 2016).

The multiple applications of AgNPs in the daily living (as AgNP dietary supplements, AgNP-coated food recipients, as alternative to antibiotics in livestock and poultry, in contaminated water and aquatic animals, in pharmaceutical products) and the increased consumers' exposure to these kind of products urge the need to perform their toxicological profile design since there were raised some concerns regarding the potential noxious effects on human health based on the fact that the mechanism of toxicity of these nanoparticles still has some gaps (Bergin et al., 2016; Hendrickson et al., 2016).

In order to preserve the biological activity, to improve stability and to reduce toxicity, different natural/synthetic polymers which are known to be well tolerated by human body are used to achieve coated nanoparticles as potential safe formulations (e.g. proteins, alginates, chitosan, polyethylene glycol, poly-*N*-vinyl pyrrolidone etc.) (Kuskov et al., 2007, 2017).

These concerns led us to the idea of obtaining stable uncoated and PEG-coated silver nanoparticles with a size that is safe after *in vitro* and *in vivo* administration. These colloids will be further used as carriers for agents with a low aqueous solubility administered in skin pathologies. Our previous studies showed that silver nanoparticles are relevant theranostic solutions for diagnostic and therapeutic surveillance in skin disorders (Ciurlea et al., 2012). An area of great interest for our research group is the application of nanotechnology to increase the solubility of active skin therapeutic compounds like pentacyclic triterpenes (Dehelean et al., 2013).

The present work was aimed: i) to synthesize stable bare and PEG-coated silver nanoparticles and ii) to assess the *in vitro* (on HaCat cells) and *in vivo* (i.p. administration to mice) acute/subacute toxicity signs, respectively. The experimental data acquired showed an efficacy/toxicity ratio of test compounds oriented predominantly towards efficacy in the light of a well-established dosage and preparation conditions setting.

2. Materials and methods

2.1. Reagents

The reagents used to prepare bare silver nanoparticles (AgNPs) and PEG-coated silver nanoparticles (PEG-AgNPs), namely silver nitrate (Merck, Germany), trisodium citrate dihydrate (Sigma-Aldrich, Germany), sodium dodecyl sulphate (SDS), (Acros Organics, Belgium), polyethylene glycol (PEG-400) (Sigma-Aldrich, Germany), were of analytical grade and used as starting materials. Milli-Q water was used as solvent throughout the experiments. The media and reagents for cell culture including Dulbecco's Modified Eagle's Medium (DMEM), fetal calf serum (FCS), saline phosphate-buffered (PBS), antibiotic mixture (penicillin/streptomycin), and trypsin-EDTA solution were purchased from Sigma Aldrich (Munich, Germany).

2.2. Cell line

The cell line used in the present study was a line of immortalized human keratinocytes - HaCat cells purchased from ATCC as frozen item.

2.3. Synthesis and characterization of AgNPs and PEG-AgNPs

The synthesis process used to prepare bare and PEG-coated silver nanoparticles was based on Turkevich's method slightly modified (Turkevich et al., 1951), as follows: silver nitrate (1 mM) was dissolved in 100 mL of deionized water (Milli-Q ultra-pure water), under magnetic stirring, at 80 °C; a mixture of trisodium citrate dihydrate (0.4 mM) and sodium dodecyl sulphate - SDS (0.5 mM) – used as capping agent in 100 mL of deionized water was dropped for 30 min under continuous stirring. The reaction mixture was kept at 80 °C, 350 rpm for 4 h, in order to reach yellow color characteristic to the AgNPs formation, and then was cooled at room temperature, stored in a dark flask and kept refrigerated. PEG-coated silver nanoparticles were obtained by adding under continuous stirring an aqueous solution of polyethylene glycol (PEG 400) to the previously obtained AgNPs colloid. The final colloid was refrigerated, protected from light until further use.

Nanoparticles formation was confirmed by the means of UV–Vis and Raman spectroscopy. UV–Vis absorbance spectra were obtained with a Cary 60 UV–Vis spectrophotometer (200–600 nm domain). Raman and surface enhanced Raman spectroscopy (SERS) spectra were acquired utilizing a LabRam HR 800 system (confocal Raman microscope - BX41, a 50x Olympus objective, a He-Ne laser, 15 mW output, a thermo-electrically cooled CCD camera). The morphology of NPs was characterized by transmission electron microscopy (TEM) using a FEI Tecnai 12 Biotwin microscope. The particle sizes and zeta potential were analyzed by photon correlation spectroscopy (PCS) using a Zetasizer Nano ZS system (Malvern Instruments, Malvern, UK). The resulting spectra were processed in the Origin 8 software.

2.4. Cell culture

The HaCat cells were cultured in specific culture medium - Dulbecco's modified Eagle Medium (DMEM) with high glucose (4.5 g L^{-1}), L-glutamine and sodium bicarbonate, supplemented with 100 U mL^{-1} penicillin, 100 μg mL^{-1} streptomycin, and 10% fetal bovine serum (FBS). The cells were cultured according to the standard conditions: a humidified atmosphere with 5% CO_2 at 37 °C and were passaged at every two-three days. The number of cells used in the experiments was determined in the presence of Trypan blue using a Neubauer counting chamber (Coricovac et al., 2017).

2.5. Cell viability assays - Alamar blue and MTT assay

For the Alamar blue assay, the HaCat cells (1×10^4/200 μL medium/well) were seeded in a 96-well plate and allowed to attach. After the cells attached to the plate, were incubated with different concentrations (0.1, 0.3, 1, 3, 10 and 50 μM) of the AgNPs and PEG-AgNPs colloids for different time points: 24, 48, and 72 h. After the incubation period, the Alamar blue reagent was mixed in a 1:10 ratio with DMEM (10% FBS) was added to each well. The plates were incubated for 3 h at 37 °C and the absorbance of each well was measured using a xMark™ Microplate Spectrophotometer (Biorad) at 570 nm and 600 nm (reference) wavelengths. Cell viability was calculated according to the formula described in our previous articles (Soica et al., 2014).

Another viability test conducted in the present study was the MTT (3- (4,5-Dimethylthiazol-2-yl)-2,5-diphenyltetrazolium bromide) assay. The culture protocol was similar to the one described for Alamar blue. Briefly, 1×10^4 cells/200 μL medium/well were seeded in a 96-well plate and allowed to attach. The cells were stimulated with multiple concentrations (0.1, 0.3, 1, 3, 10 and 50 μM) of the AgNPs and PEG-AgNPs solutions for 24, 48, and 72 h. The MTT reagent (10 μL) was added and incubated for 3 h. The resulting purple crystals were dissolved in solubilization buffer (100 μL) and spectrophotometrically analyzed at 570 nm using a microplate reader (xMark Spectrophotometer - BioRad).

2.6. In vivo toxicity protocol

SKH-1 adult male hairless mice, weighting: 30–35 g (Crl: SKH1-*Hr*^{hr}, Charles River Laboratory, Budapest, Hungary) were used for the *in vivo* experiments. The mice were acclimatized to the laboratory conditions for two weeks before the experiment. They were kept in the University

animal facility under standard conditions: 12 h light/dark cycle and free access to food and water. The experimental procedures and protocols were in agreement with the European Directive 2010/63/EU, the AVMA (American Veterinary Medical Association) Guidelines for the Euthanasia of Animals (2013 Edition) and the National Law 43/2014 regarding the protection of animals used for scientific purposes and were approved by the University Research Ethics Committee. The acute/subacute toxicity following i.p. administration was tested according to the OECD guideline 420 principles. The animals were divided in four groups (n = 10 mice/group): group 1 – control group (no interventions), group 2 – mice that received 10 mg/kg body weight of media (trisodium citrate and SDS solution) i.p. daily (6 days), group 3 - mice that received 10 mg/kg body weight of AgNPs i.p. daily (6 days), and group 4 - mice that received 10 mg/kg body weight of PEG-AgNPs i.p. daily (6 days). Five mice from each group were euthanized at three hours after the first i.p. administration, the rest being euthanized at the end of the experiment, under anesthesia by using Isoflurane as inhalator anesthetic, followed by manual cervical dislocation. Changes in mice weights, behavioral pattern (salivation, tremors, lethargy, sleep and coma) and skin appearance were the assessed parameters.

2.7. Non-invasive skin parameters measurements

A non-invasive technique was applied for the measurement of the skin physiological parameters (skin hydration, melanin, and erythema). The equipment used was an electronic Skin Colorimeter CL 400 and the Corneometer®CM 825 (Courage-Khazaka, Koln, Germany). The Skin Colorimeter CL 400 principle is based on the tristimulus colorimetry. The results are expressed by the means of the standard color Commission International d'Eclairage (CIE) Lab system in which colors are described by their lightness value (L*), the amount of green or red (a*), and the amount of yellow or blue (b*) they contain (Taylor et al., 2006). L* measured skin reflectance or lightness (a grey scale with values ranging from 0 to 100, where 0 is black and 100 is white); a* measures the color saturation from red to green (scale from +60 to −60, where positive values indicate varying intensities of red); b* measures the color saturation from yellow to blue (a scale +60 to – 60, where positive values indicate varying intensities of yellow) (Alaluf et al., 2002). The L*a*b* parameters were expressed as arbitrary units. The hydration of the stratum corneum was determined using the Corneometer®CM 825 probe (Coricovac et al., 2017).

2.8. Biochemical analysis

In order to evaluate the changes in blood circulating system, samples were collected at three hours after first administration and at the end of experiment - day 6. Blood samples were collected on serum clot activator tubes for serological analyses (IL ILab 650 Chemistry Analyzer) and into potassium EDTA-coating tubes for hematological analyses (Sysmex SF 3000 Automated Hematology Analyzer). The following blood parameters were measured: white blood cells count (WBC), red blood cells count (RBC), hemoglobin (HGB), hematocrit (HCT), mean corpuscular volume (MCV), mean corpuscular hemoglobin (MCH), mean corpuscular hemoglobin concentration (MCHC), red blood cell distribution width (RDW), platelets count (PLT), and mean platelet volume (MPV). The serum parameters measured were: alanine transaminase (ALT), aspartate transaminase (AST), blood urea nitrogen (BUN), and creatinine (CR).

2.9. Histopathological evaluation

An early assessment of the organs was performed at three hours after i.p. injection and half of the mice from all four groups were sacrificed for histopathological analysis. The second mile stone was considered in the sixth day of the experiment when the rest of the mice were euthanized, also after three hours from last intraperitoneal injection. All animals used in this study were sacrificed under anesthesia by inhalation using Isoflurane followed by cervical dislocation, the procedures being realized according to the AVMA Guidelines for Euthanasia. At both time points, clinically normal skin and organs (heart, kidney, liver, lung, and spleen) were harvested from all the mice, weighed and fixed in 4% v/v buffered formaldehyde and embedded in paraffin. Sections of three micrometer thickness were obtained using a Leica Rotary Microtome RM2255 and stained with hematoxylin and eosin (H&E) using the standard histopathological technique. The microscopic examination was conducted using a Leica Light Microscope DM750 and images were captured using a Leica DMShare System.

The distribution (superficial *vs.* reticular dermis), number (as mean value of 20 randomly picked high power fields) and size (as mean value of 50 cells diameter) of the mast cells at skin level were evaluated in each case. Changes in the internal organs compared to the control mice were also noted.

2.10. Statistical analysis

Graph Pad Prism 5 and Origin 8 software were used for the presentation and interpretation of the results. The results were expressed as the mean ± standard deviation. One-way ANOVA analysis was applied to determine the statistical differences followed by Tukey post-test (*$p < 0.05$; **$p < 0.01$; ***$p < 0.001$).

2.11. Compliance with ethics requirements

Authors declare that the protocol involving animals complied with the specific regulations and standards; this experiment was evaluated and approved by the Ethics Committee of the "Victor Babes" University of Medicine and Pharmacy Timisoara, Romania.

3. Results

3.1. Characterization of bare and PEG-coated silver nanoparticles

The approach that was applied concerning Turkevich's method by adding sodium dodecyl sulphate – SDS (as capping agent to control size and stability) together with trisodium citrate dihydrate (as reducing agent) and silver nitrate (as metal precursor) proved to be successful, the first indication being the apparition of the yellow color characteristic for silver nanoparticles formation. Subsequently were performed microscopic and spectroscopic tests to confirm the findings. Size distribution measurements revealed that both AgNPs and PEG-AgNPs had narrow size distributions with mean hydrodynamic sizes with an average of 19 nm and 50 nm (DLS), respectively.

TEM images showed that the majority of AgNPs have spherical shapes with faceted nanoparticles whereas PEG-AgNPs presented a small electron dense core surrounded by a relatively circular halo (Fig. 1). TEM size histogram showed that AgNPs and PEG-AgNPs had diameters between 0 - 45 nm and 15–55 nm size range, respectively.

Zeta potential values were found to be −40 mV for AgNPs and −37 mV for PEG-AgNPs, thus indicating a high stability of the colloidal system.

The SPR peaks detected at 435 nm and 425 nm in the UV–Vis absorption spectra are indicative of the formation of AgNPs and PEG-AgNPs, respectively (Fig. 1). The broad profile of the absorption bands of PEG-AgNPs may be attributed to a larger size distribution and possibly due to the presence of some PEG-AgNPs and PEG-AgNPs-aggregates of other shapes. In fact, the PEG-AgNPs colloid exhibited a second very broad peak at about 650 nm. Vibrational modes characteristic to PEG were observed in the colloidal PEG-AgNPs samples at 439, 544, 842, 897, 953, 1071, 1136, 1252, 1287, 1476, and 2718-2958 cm^{-1} suggesting the PEGylation of AgNPs (Fig. 1) (Koenig and Angood, 2003; Djaqued et al., 2005; Yamini et al., 2014). The SERS

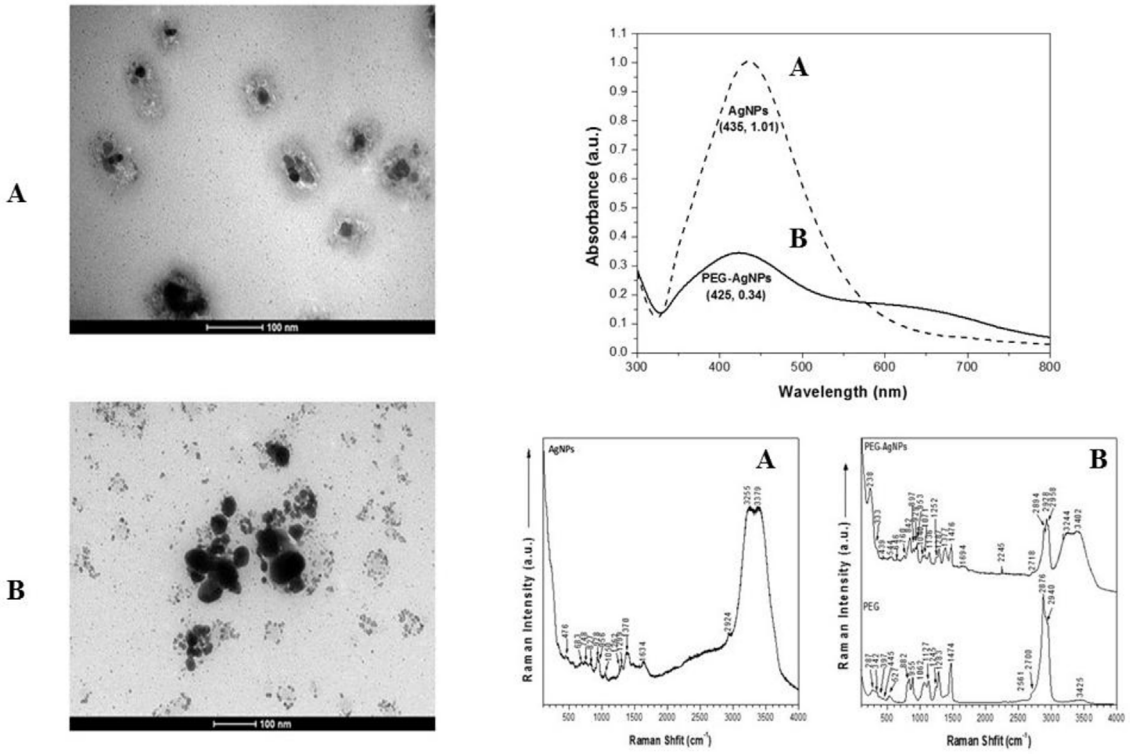

Fig. 1. TEM images of AgNPs-A and PEG-AgNPs-B; UV–Vis absorption spectra of the two aqueous colloids - the corresponding wavelengths and related intensities (arbitrary units) of the SPR peak are mentioned in brackets; Raman spectra collected from the colloidal AgNPs and PEG-AgNPs using a 632.8 nm excitation line and a 20 s acquisition time (spectra averaged over $n = 3$ cycles). The Raman spectra of sodium dodecyl sulphate and PEG were inserted as controls.

peaks are shifted by up to $\sim 20\ cm^{-1}$ from the corresponding ones in the Raman spectrum of the control PEG alone (Fig. 1). This is not uncommon in SERS, when molecules chemisorb to the nanosurface and experience an increase in signal at lower concentrations. Reference Raman database of pharmaceutical excipients (de Veik et al., 2009) showed that the Raman spectrum of the AgNPs colloid presented vibrational modes characteristic to SDS at 827, 928, 1050, 1299, 1370, and 2924 cm^{-1}.

3.2. Cytotoxicity assessment

In order to evaluate the cytotoxic effects of bare and PEG-coated silver nanoparticles on normal human keratinocytes – HaCat viability, there were tested different concentrations (0.1, 0.3, 1, 3, 10 and 50 μM) of the test colloid nanoparticles for different time points (24, 48 and 72 h). The results obtained indicated that at the lowest concentrations tested (0.1, 0.3, 1 and 3 μM) the number of the viable cells was not affected by the nanoparticles addition, neither at 24 h nor after 72 h stimulation. These data were confirmed by both Alamar blue and MTT assays (data not shown). The solutions of trisodium citrate and sodium dodecyl sulphate (used in the synthesis process) were tested as positive controls; no changes were detected in terms of cells viability as compared to control cells (unstimulated cells) (data not shown). At the highest concentrations tested - 10 and 50 μM, there were observed significant cytotoxic effects induced by the nanoparticles (AgNPs and PEG-AgNPs), the most significant effect being recorded after stimulation with 50 μM and a longer stimulation time (48 and 72 h) (Fig. 2).

3.3. Clinical and general signs

In this acute/subacute toxicity experiment, no death was recorded in the six days of observation time in all groups (control and treated mice). There were no significant changes in the general appearance, but some differences in the percentage of weight between the groups were

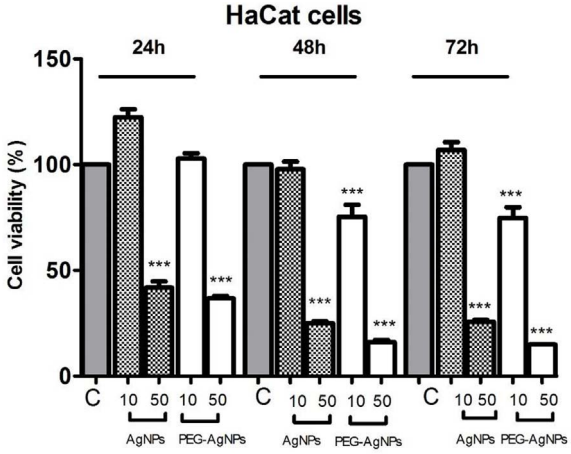

Fig. 2. Cytotoxic effect of AgNPs and PEG-AgNPs on human keratinocytes – HaCat cells related to control cells (unstimulated) based on Alamar blue assay. All experiments were performed in triplicate, the results are presented as mean values ± SD, and the statistical test used was One-way ANOVA and p values were: *$p < 0.05$, **$p < 0.01$, ***$p < 0.001$.

detected.

Biochemical analysis of plasma was achieved to assess hepatic (ALT, AST) and renal health status (BUN, CR). Alanine transaminase (ALT) and aspartate transaminase (AST) were employed as indicators of hepatic function; urea and creatinine were indicators of the renal function. Table 1 summarizes the values obtained for the different groups. As it can be observed no significant changes in urea and creatinine levels were observed in any group, while ALP and AST remain in normal levels (Table 1). The hematological analysis showed no significant changes of WBC, RBC, HGB, HCT, and PLT and also for MCV, MCH, MCHC, RDW, PDW, and MPV (see supplementary material) in

Table 1
Effect of test compounds on serological parameters in mice groups at three hours and at six days (n = 5; mean ± S.D.).

Time	Groups	ALT (U L^{-1})	AST (U L^{-1})	BUN (mg dL^{-1})	CR (mg dL^{-1})
3 h	Control	42 ± 2.8	32 ± 5.8	27 ± 10.3	0.9 ± 0.09
	Media	47 ± 3.2	39 ± 7	36 ± 6.2	1.1 ± 0.15
	AgNPs	38 ± 6.1	24 ± 10	32 ± 6.1	0.9 ± 0.07
	PEG-AgNPs	19 ± 7.8	28 ± 5.1	22 ± 6.3	1.0 ± 0.05
6 days	Control	44 ± 4.6	12 ± 7.2	26 ± 7.2	0.7 ± 0.08
	Media	36 ± 5.3	31 ± 4.8	40 ± 11.6	1.1 ± 0.08
	AgNPs	17 ± 10.8	19 ± 15.2	31 ± 9.8	1.2 ± 0.11
	PEG-AgNPs	38 ± 8.4	25 ± 7.9	23 ± 12.9	0.8 ± 0.19

mice treatment groups compared to the control groups.

3.4. Non-invasive measurements

In order to evaluate the *in vivo* toxicity of the colloidal solutions of AgNPs and PEG-AgNPs after i.p. administration to healthy SKH-1 hairless mice, were also assessed the evolution of body weight and the impact of these nanoparticles at skin level due to their use as potential nanocarriers for skin treatment and diagnostic.

Our data indicated that administration of the AgNPs and PEG-AgNPs was associated with a significant increase of the body weight as compared to control group, whereas in the case of the mice that received media it was noted a decrease of this parameter. These changes were significant mainly in the first 96 h (Fig. 3), after the last two doses, the values were closed to the ones recorded for the control group (data not shown).

The skin hydration measurements showed decreased values of this parameter after the second dose post-administration of all three test solutions (AgNPs, PEG-AgNPs and media) as compared to control group. After the administration of the last dose, the values seemed to increase in all groups of mice, these data being devoid of statistical significance (see Supplementary material).

The tristimulus colorimetry principle provides data regarding the changes in physiological skin parameters (melanin and erythema), changes that represent key markers in the diagnostic of skin pathologies. The negative values of L* and the positive values recorded for a* in all the groups of mice were associated with the presence of erythema after the administration of AgNPs, PEG-AgNPs and media (Fig. 4A). In the groups of mice that received AgNPs and PEG-AgNPs was observed a decrease of L* and an increase of b* what could be explained by the presence of pigmentation (Fig. 4B). In Fig. 4A and B were described the significant variations observed between the groups in the first 96 h, whereas the values recorded during the last two days of experiment presented a linear trend without statistical significance (data not shown).

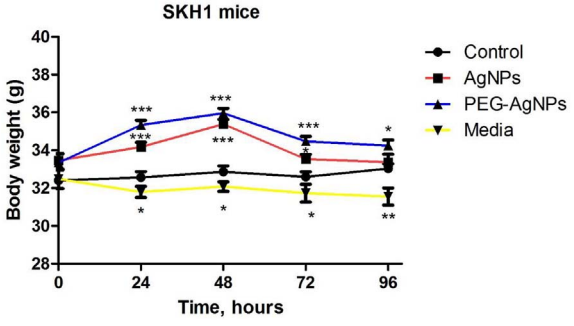

Fig. 3. Body weight evolution of the mice. The results are presented as mean values ± SD. The statistical test used was One-way ANOVA and p values were: *p < 0.05, **p < 0.01, ***p < 0.001.

3.5. Histopathological aspects

Microscopic evaluation of the skin specimens from the control group mice, both time, three hours and six days respectively, showed normal histology of the epidermis and dermis, with small mast cells filled with basophilic granules, distributed in all levels of the dermis (Fig. 5a). The diameter of the mast cells was 0.0203 mm and the number as 16.1 (Table 2).

At three hours after first media administration, there was an increase in the number (20.5 versus 16.1 in control group) and diameter of the mast cells, 0.0280 mm versus 0.0203 mm, in control group (Fig. 5b, Table 2). Even if the mast cells were bigger than those observed at control group mice, they were degranulated, with many granules released in the surrounding extracellular space. The mast cells were distributed around blood venules and arterioles of deep vascular plexus (Fig. 5b).

The mice sacrificed in the sixth day of the experiment at three hours after media i.p. administration, presented a similar number of mast cells as control group (15.7 *vs.* 16.1 in control group), but the diameter of the mast cells was bigger in these cases compared with control group and even with those mice euthanized at three hours after first intraperitoneal administration, 0.0354 mm *vs.* 0.0280 mm at three hours and 0.0203 mm in control group (Fig. 5c, Table 2).

Both media treated mice groups, those euthanized at 3 h after first i.p. administration and those euthanized in the sixth day of the experiment, at three hours after last i.p. administration, showed mast cells distributed with predilection in perivascular spaces (Fig. 5b and c).

At three hours after first AgNPs i.p. administration, the mast cells were distributed mainly around the blood vessels of the dermal profound vascular plexus (Fig. 5d). The size of mast cells increased compared to control group or media treated group, being similar with the values observed at three hours after last media administration, 0.0343 mm *vs.* 0.0203 mm in control group and 0.0354 mm in media treated mice group, at the end of the experiment (Fig. 5d, Table 2). The number of the mast cells decreased from 16.1 in control group at 11.6 (Table 2).

At the end of the experiment, the mice treated with AgNPs presented deep situated mast cells, around blood vessels (Fig. 5e). The diameter of the mast cells was similar to that noticed in control group, 0.0249 mm versus 0.0203 mm in control group (Table 2). Similar to the data observed at three hours after first AgNPs administration, at the end of the experiment the number of the mast cells noted at dermal level decreased compared to the normal, but even with that observed after first administration of AgNPs, 8.1 *vs.* 16.1 at control group and 11.6 after first administration of AgNPs (Fig. 5e, Table 2).

At three hours after first administration of PEG-AgNPs, the mice presented mast cells distributed at all levels of the dermis, similar to that observed in control group (Fig. 5f). The size of mast cells increased at 0.0277 mm *vs.* 0.0203 mm in control group, but similar to the value observed in the media treated group at the same time of the experiment (0.0280 mm) and lower than the diameter noted in AgNPs treated group, 0.0343 mm (Table 2). The number of the mast cells was similar to that noted at the same time of the experiment in the AgNPs treated group, 11.8 *vs.* the 11.6 in AgNPs group (Fig. 5f, Table 2).

The skin specimens harvested from the mice treated with PEG-AgNPs at the end of the experiment, showed a slight increasing in the size of the mast cells compared to the samples harvested from the same group, at three hours after first administration, 0.0308 mm *vs.* 0.0277 mm, and were bigger than those observed at the control group, 0.0203 mm (Table 2). Also, the number of mast cells decreased slightly at 11.3 from 11.8 mast cells after first administration (Fig. 5g, Table 2). The mast cells showed no predilection for any part of the dermis, being distributed at all levels (Fig. 5g).

At all mice groups, the epidermis and dermis showed quasinormal architecture. Moreover, only minimal hyperemia of venules and arterioles of deep vascular plexus was observed (Fig. 6). In the group treated

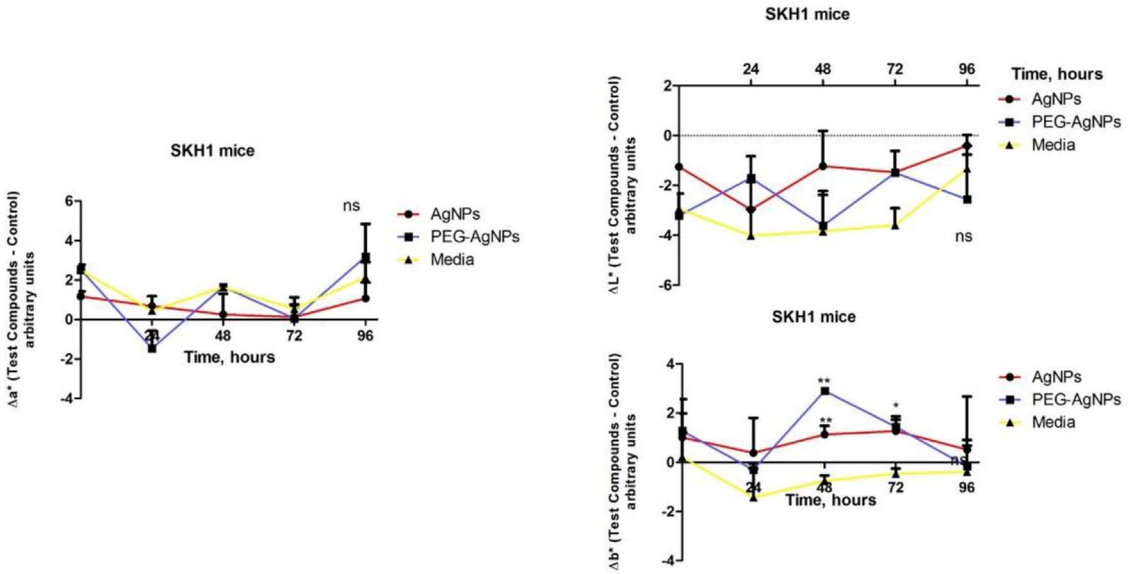

Fig. 4. Physiological skin parameters evolution: A. Melanin-related measurements (values expressed as ΔL* and Δb*) and B. Erythema-related measurements (values expressed as Δa*), where Δ – is the difference between the mean value of the test groups obtained for L*, b* and a* (for each time point) and the mean value for this coordinate in the control group (no interventions applied). The results are presented as mean values ± S.D. ** indicate significant differences between control at $p < 0.01$ and * at $p < 0.05$.

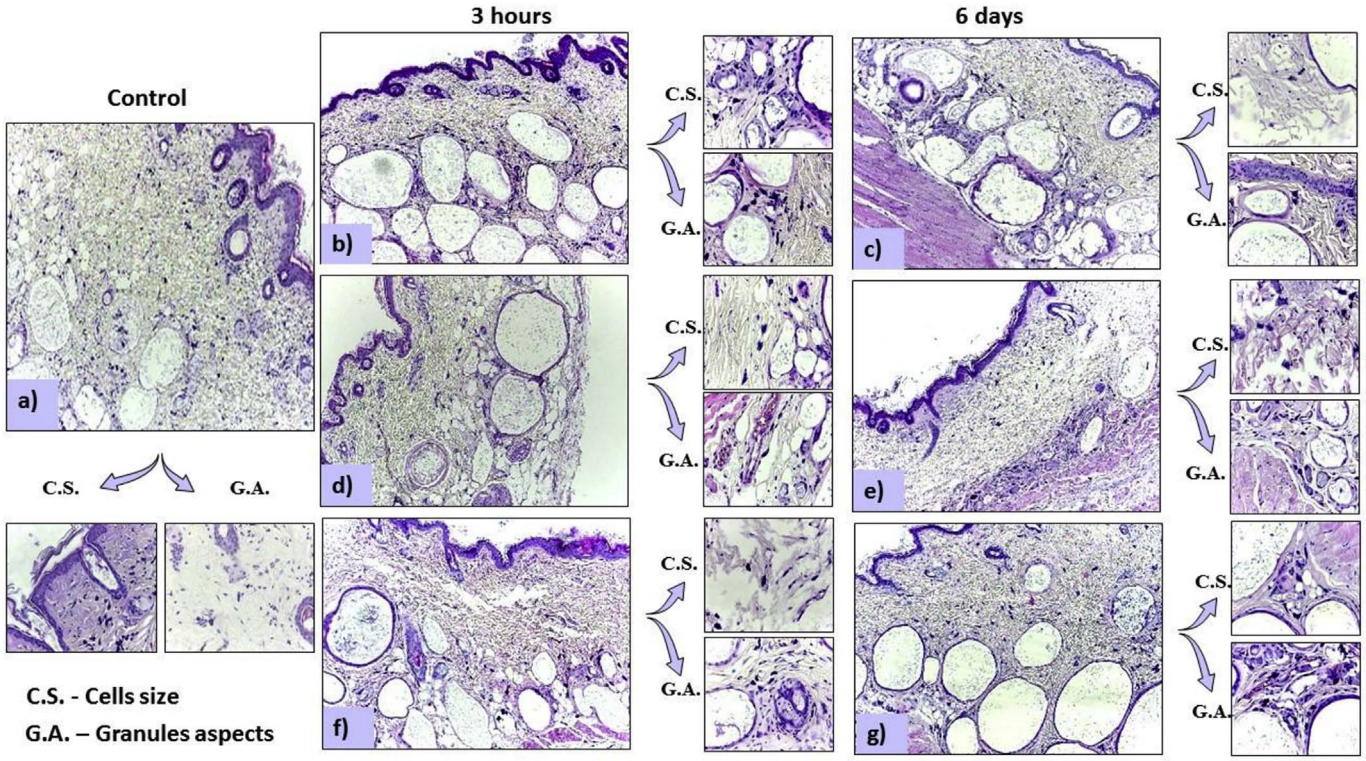

Fig. 5. Histological aspects of the skin specimens (H&E stain). Distribution of the mast cells mainly at dermal level, original magnification (OM) x10; cells size and granules aspects, OMx40; a – control group, b – mice treated with media, euthanized after 3 h from the first i.p. administration, c - mice treated with media, euthanized in the 6th day at 3 h after the last i.p. administration, d – mice treated with AgNPs, euthanized after 3 h from the first i.p. administration, e - mice treated with AgNPs, euthanized in the 6th day at 3 h after the last i.p. administration, f – mice treated with PEG-AgNPs, euthanized after 3 h from the first i.p. administration, g - mice treated with PEG-AgNPs, euthanized in the 6th day at 3 h after the last i.p. administration.

with AgNPs, after first administration, the blood vessels of deep vascular plexus showed leukocytes margination (Fig. 6d). On the skin specimen harvested after PEG-AgNPs first administration, the blood vessels showed marked hyperemia that decreased in intensity until the end of the experiment (Fig. 6f and g).

No major differences were observed between control group and treated mice internal organs histology, neither if the specimens were harvested at three hours after first intraperitoneal injection, nor after six days of experiment. All mice showed minimal deviation of normal histology of heart, lung, kidneys and spleen, with small quantity of interstitial edema and vascular hyperemia (see Supplementary material).

Table 2
The mean values for size and number of mast cells.

Mast cells	Size[b] (mm)		Number[c]	
	3 h	6 days	3 h	6 days
Control group	0.0203	0.0203	16.1	16.1
Media[a]	0.0280	0.0354[d]	20.5[d]	15.7
AgNPs	0.0343[d]	0.0249	11.6	8.1[d]
PEG-AgNPs	0.0277	0.0308	11.8	11.3

[a] Media – solution of trisodium citrate and sodium lauryl sulphate used to deliver bare and coated silver nanoparticles.
[b] Size was calculated as mean value of 50 cells diameter.
[c] Number of mast cells was calculated as mean value of 20 randomly picked high power fields.
[d] Important changes.

4. Discussions

The present study was aimed to characterize the synthetized bare and PEG-coated AgNPs *in vitro* effects on non-tumorigenic (HaCat) cells and *in vivo* after i.p. administration to SKH-1 hairless mice from a toxicological perspective. The bare and PEG-coated AgNPs obtained in this study will be further used as carriers for anticancer drugs for skin disorders and their own toxicological profile had to be tested.

The physico-chemical features (size, shape, surface charge, coating, *etc*.) of the NPs play crucial roles in the interactions between the nanoparticles and the immune system, and a large number of specific mechanisms of action takes place, from protein binding to biological corona formation (Neagu et al., 2017; Piperigkou et al., 2016; Engin et al., 2015). In order to obtain a reliable drug delivery system for nanomedicine field, all the mechanisms involved need to be fully elucidated and understood.

Several methods were developed to obtain silver nanoparticles, such as: reduction (photolytic, radiolytic, solvent extraction, organic solvent), sonication, microemulsion, polyol and alcohol processes, but one of the most frequently employed method to synthesize AgNPs is the chemical reduction (Mendis et al., 2016). Chemical reduction is a common term use to describe the method applied for obtaining silver nanoparticles. This process takes place in solvent media and the final product is a colloid. The mechanism involved is a complex one based on the numerous phenomena implied – reduction, nucleation, growth, coarsening, agglomeration – that occur during co-precipitation synthesis (Pacioni et al., 2015). This method provide a control over the particle size and behavior of the nanoparticles obtained which play a crucial role in compounds toxicity. Different compounds, such as: citrate, PEG, PVP, proteins etc. are used as coatings in order to promote stability, avoid aggregation of AgNPs, to decrease interactions between the blood proteins and to obtain a prolonged blood circulation (Bastos et al., 2016; Soica et al., 2016). Polyethylene glycols having a low molecular weight are well known for a number of advantages, among which: food additives permitted for direct addition to food for human consumption; good cosolvents (being regarded as protic solvents with aprotic sites); widely used as pharmaceutical excipients (e.g. PEG-protein conjugate selected NP-based drug approved by the FDA for leukemia) (CFR, 2017; Maryamabadi et al., 2016; Najafi-Hajivara et al., 2016). PEG 400 does not possess adjuvant activity and has been successfully used for: a novel polyethylene glycol mediated lipid nanoemulsion as drug-delivery carrier for paclitaxel; pore-forming and plasticizers in the capsule shells contain active drug; coated AgNP in order to decrease the affinity for protein interaction with it own surface and thus retained significant amount of inherent bactericidal activity etc. (Larsen et al., 2002; Jing et al., 2014; Liu et al., 2014; Ban and Paul, 2016).

Regarding synthesis of bare and PEG-coated AgNPs, citrate is used as reductant and capping agent, SDS as stabilizer and size controller, while PEG for the ability to control the processes involved (nucleation and growth) in a temperature-dependent manner. Bare AgNPs are stabilized by charge repulsion while PEG-coated AgNPs are sterically stabilized (Sharma et al., 2014).

Thus, the AgNPs and PEG-coated AgNPs colloids characterized in this study were synthetized by using Turkevich's method, the addition of sodium dodecyl sulphate (SDS) as stabilizer and size controller, represented the modification implemented to the classic method. As a result, it could be stated that it was standardized a protocol that requires around 4 h to obtain a stable AgNPs solution, the yellow color that was obtained being a marker of the stable nanosized silver particles formation.

According to the literature, silver nanoparticles form colored colloids, from pale yellow to dark brown, due to the surface plasmon

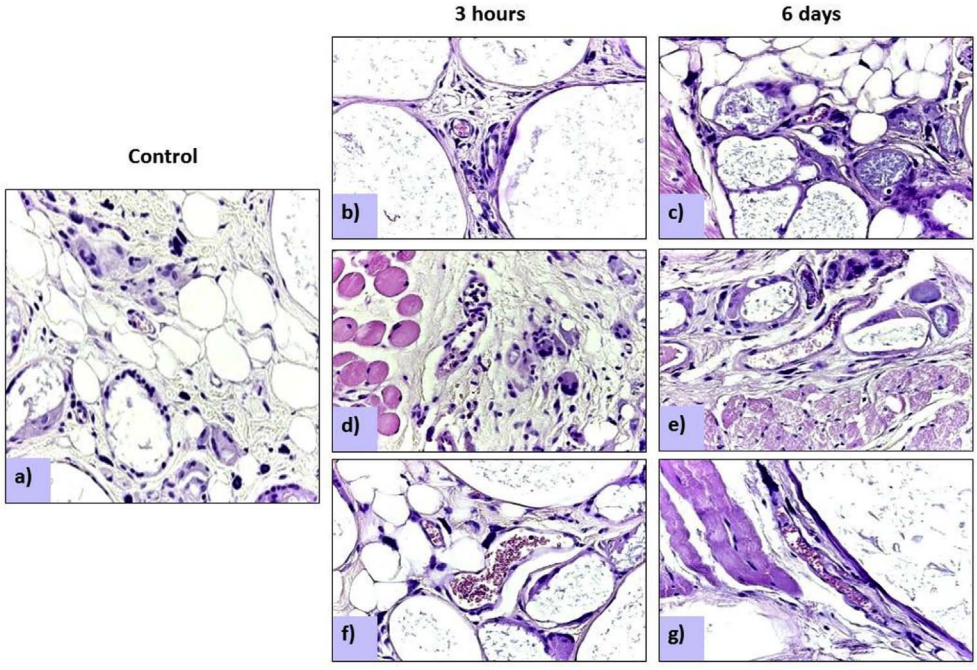

Fig. 6. Histological aspects of the skin specimens, H&E stain. Aspects of leukocyte margination (d) and deep vascular plexus, with hyperemia of the blood vessels (f), OMx40; a – control group, b – mice treated with media, euthanized after 3 h from the first i.p. administration, c - mice treated with media, euthanized in the 6th day at 3 h after the last i.p. administration, d – mice treated with AgNPs, euthanized after 3 h from the first i.p. administration, e - mice treated with AgNPs, euthanized in the 6th day at 3 h after the last i.p. administration, f – mice treated with PEG-AgNPs, euthanized after 3 h from the first i.p. administration, g - mice treated with PEG-AgNPs, euthanized in the 6th day at 3 h after the last i.p. administration.

resonance (SPR) in the UV–Vis area (300–600 nm) and the silver nanoparticles that are yellow in color seem to be the most stable ones, data that are in agreement with the results described in this article (Mendis et al., 2016; El-Zahry et al., 2015). During the growth process, a broad band of low intensity indicated the presence of small nanoparticles; as the nanoparticles grew bigger, the absorption bands became narrower and increased in intensity. The broad profile of the absorption bands may be attributed to the NP's aggregation or/and the adsorption of organic species at their surface. The bare and PEG-coated silver nanoparticles display a similar size and spherical shapes as indicated by the wavelengths of their absorption bands (425 and 435 nm, respectively) confirmed also by the TEM analysis.

TEM micrographs also displayed nanoparticles being non-uniform in size and shape, disposed as individual entities as well as aggregates, due to the assembly of smaller particles. Within the aggregates, individual nanoparticles were not in direct contact with each other, thus indicating higher stability through the use of a capping agent (surfactant, PEG) (Saifuddin et al., 2009). In spite of the fact that AgNPs shaped as discs or rods exhibit more appropriate properties for blood circulation than spherical AgNPs, the latter provide a faster cellular uptake presumably due to more suitable binding properties to the target sites (Muhamad et al., 2014) and are more thermodynamically stable (Muhammad et al., 2016). The shape of the AgNPs is also a very important parameter in terms of evaluating the possible interactions with the cells within the body, the spherical form being recommended for the use in medical fields due to a reduced toxicity associated with their administration (Wei et al., 2015). Sharma et al. studied coated NPs in biological media, and their findings showed important changes for citrate-coated AgNPs (from spherical to triangular and hexagonal shapes) while PEG-coated AgNPs spherical shape does not suffer any changes (Sharma et al., 2014).

Surface modification, surface charge and polymer type have some influence regarding both type of biological activity correlated with toxicity *in vitro* and *in vivo* assessment. Some studies demonstrated that the toxicity of AgNPs on murine hepatoma cells depended on the surface chemistry of nanoparticles and PEG-coated exerts a better biocompatibility, with an adequate biological inertia, which is materialized in effective opsonization resistance and/or non-specific binding to protein in animal model, also with reduced toxicity on embryonic fibroblasts (Pang et al., 2016; Caballero-Díaz et al., 2013). A high interest was attributed to the size of AgNPs that were applied in biomedical fields, since it was observed an inverse correlation between the size of the nanoparticles and the degree of toxicity induced (Chaloupka et al., 2010; Wei et al., 2015; Riaz Ahmed et al., 2017). Different studies demonstrated that smaller particles (lower than 15 nm) induced higher toxicity compared to bigger ones (20–100 nm) (Engin et al., 2017). Thus, Gliga et al. showed that 10 nm AgNPs were cytotoxic for human lung epithelial normal cells, without no difference in toxicity regarding the coating type (citrate or PVP); Liu et al. proved that 5 nm AgNPs were more toxic than 20 and 50 nm AgNPs in four tumor cell lines; Kang et al. showed that 5 nm AgNPs induced granule release, increase the level of intracellular calcium ions generating oxidative stress at subtoxic concentrations (Gliga et al., 2014; Kang et al., 2017).

The results obtained during the synthesis and characterization of the bare and PEG-coated AgNPs indicated that there were achieved stable nanoparticles with an average size of 19 (for AgNPs) and 50 (for PEG-AgNPs) nm, data that are in agreement with the information from the literature stated above. Silver nanoparticles that have a size lower than 10 nm are highly reactive determining lesions at cellular level, whereas the size range between 20 and 100 nm did not affect the integrity of the cells (Williams et al., 2016; Ivask et al., 2014).

One of the most important parameter in the biomedical use is the stability of nanoparticles (Mandal et al., 2011; Ban and Paul, 2016). A highly negative or positive value of the zeta potential indicates a strong repulsion between colloidal particles and, subsequently, the lack of flocculation tendency. Particles having a zeta potential more positive than +20 mV or more negative than −20 mV are typically considered to be stable due to the repulsion among the particles preventing agglomeration (Phongtongpasuk et al., 2016). Zeta potential data (−40 mV for AgNPs and −37 mV for PEG-AgNPs) recorded in the present study are in accordance with the results from the literature and indicate that the nanoparticles obtained are stable.

In order to assess the *in vitro* effects on cell viability of the stable bare and PEG-coated AgNPs, there were employed standard and reliable assays, Alamar blue and MTT. The cell viability assessment *in vitro* techniques offer valuable information regarding the toxicological endpoints induced by the administration of different agents or nanomaterials in terms of cell mortality, biochemical and physiological changes (Ciappellano et al., 2016). All new compounds including metallic nanoparticles must comply with the preclinical *in vitro* screening that includes the aforementioned *in vitro* cell viability assays.

The results concerning the cytotoxic effects of bare and PEG-coated silver nanoparticles evaluated at 24, 48 and 72 h on human normal keratinocytes – HaCat, indicated a lack of toxicity at concentrations lower than 10 μM, whereas higher concentrations (50 μM) induced a significant rate of mortality at all three time points (Fig. 2). Jiravova et al., demonstrated in a recent study that stimulation of SVK 14 (human keratinocytes) and NIH 3T3 (mouse fibroblasts) led to a decrease of the cells viability starting from a concentration of 13 mg L^{-1} (Jiravova et al., 2016). Silver nanoparticles proved to be cytotoxic on murine macrophages – J774A.1 at doses higher than 10 μg mL^{-1} (Nguyen et al., 2016). PEG-coating AgNPs showed a lesser degree of toxicity to HaCat cells as compared to citrate coated and the bare AgNPs (Bastos et al., 2016).

Many authors tried to establish the sensitivity of different cells to AgNPs. They tested bare and coated AgNPs in either citrate, PVP or PEG (Tejamaya et al., 2014; Ragaseema et al., 2012). Some of the authors agreed that the surface modification with polymers decreased the toxicity of AgNPs on healthy tissues (Petrov et al., 2016). Ragaseema et al. demonstrated the lack of a cytotoxic effect of PEG-AgNPs on endothelial cells and smooth muscle cells at low concentration (0.1%), with an important increase of the number of apoptotic cells when the concentration was 0.2%, because of the important cytoskeletal damage (Ragaseema et al., 2012).

For a thorough characterization of the toxicological profile of bare and PEG-coated AgNPs, it was verified the potential acute/subacute toxicity of these colloids after i.p. administration (a single dose and six consecutive daily doses) to SKH-1 hairless male mice.

The selection of the route of administration for the test substances to laboratory animals is considered to be a decisive component when establishing the experimental design and the dosing methodology, mainly because of the ethics concerns, but also for the provision of accurate data regarding the pharmacokinetics and pharmacodynamics parameters. The injection into the peritoneal cavity (i.p. route of administration) is considered to be a frequently used route of administration for small animals, presenting some advantages relative to the intravenous route, namely: administration of larger volumes of liquid active agents' formulations, an easy access to the point of injection, and in terms of bioavailability it can be said that presents similarities with the oral administration pharmacokinetics (Turner et al., 2011).

Regardless to the site of administration, the target organs for AgNPs toxicity seem to be liver and kidney, because of their accumulation at those levels, through macrophage opsonization. There were also reported signs of toxicity after AgNPs administration at skin level consisting in argyria combined with oxidative damage on cellular area. These observations are transferred on bacteria, cells, aquatic species and rodents for bio-balance tests (McShan et al., 2014). Few data are available about skin morphology after i.p. administration of bare or PEG-coated nanoparticles.

Comparative tests showed that bare AgNPs and silver nitrate ($AgNO_3$) exhibit similar levels of toxicity which can be reduced by coating with hydrophilic polymers that are also used in order to

improve stability within biological environments (Petrov et al., 2016; Zook et al., 2012). Surface coating with hydrophilic polymers such as PEG provide the nanoparticles (NPs) the ability to avoid opsonization and macrophage capture; thus a stealth system can be obtained with a longer blood circulation time (Chandran and Thomas, 2015).

The chosen dose for the i.p. administration was 10 mg/kg body weight, this dose representing the 2000x of the EPA (Environmental Protection Agency) oral reference dose – the upper limit of potential acute exposure in humans (Bergin et al., 2016; Varner et al., 2010).

Blood samples were collected at three hours after the single dose and at the same time point after the last dose of the six consecutive daily doses, analyzed in terms of hematological and biochemical parameters and no significant changes were recorded. It is known that nanoparticles and other examples of nanostructures produce dose-dependent hemolysis and blood clotting. Is relevant that each type of blood cells interact different and dependent, also, on size and charge of nanosilver materials. It was stated that silver nanoparticles determine the reduction of RBC at 500 ppm, but at lower concentrations are well tolerated. The main process involved is cell membrane destruction. Higher concentrations of product influenced blood mononuclear cells (Ataei, 2016). Nanosilver structures determine changes in “white line” of cell because of the increasing of inflammatory process (Pulit-Prociak et al., 2015). Our results indicated a well-tolerated dosage with reduced changes in all types of blood cell lines, underlining the fact that low concentrations of the tested nanoparticles induce a reduced toxicity degree.

In order to assess the effect of bare and PEG-coated AgNPs at skin level, a non-invasive method was applied to observe the changes that occurred into the skin physiological parameters values – skin hydration, melanin content (pigmentation) and erythema. Our data showed that i.p. administration of the media (trisodium citrate) solution, bare and PEG-coated colloidal solutions induced a slight change in the skin hydration values after the first doses, but until the end of experiment the values were in the same range as the values measured for the control group (see Supplementary material). It was demonstrated that some adverse reactions associated with silver compounds administration, like: argyria at skin level could appear even after drinking water contaminated with this type of compounds. The skin hydration could be considered a parameter of safety because of the demand of no changes in hydration degree (Lansdown, 2010). Our data showed that i.p. administration of the bare and PEG-coated AgNPs did not induce disturbances in hydration status of the skin.

SKH-1 hairless mice are an unpigmented and immunocompetent strain (Benavides et al., 2009). According to a previous study, the skin of adult SKH-1 mice seemed to be nonpigmented (the specific melanin staining Fontana-Masson-positive in the epidermis was absent and the melanocyte marker Mel-5 was unexpressed), albeit in the neonatal SKH-1 skin were identified melanoblasts (Man et al., 2014). On this basis, it could be stated that the presence of pigmentation (Fig. 4B) recorded in the groups of mice that received AgNPs and PEG-AgNPs was a result of the colloidal solution administration, and could be associated with the fact that these solutions were distributed in the whole mouse body and some deposits were present at skin level. Melanin granules in the skin may protect against argyria, and, also, some signs of toxicity should be considered, such as, the release of silver after hepatic metabolisation. Melanocyte function and melanogenesis are influenced by silver particles and no large variability of Mexameter values indicate also a safety profile (Lansdown, 2010). Our data are in agreement with the data from the literature which affirm that skin is one of the organs where silver can be detected after parenteral administration (Arora et al., 2012; Lankveld et al., 2010). It was mentioned that an elevation of silver in blood led to a blue or grey discoloration of the skin due to the accumulation at this level, status known as argyria (Arora et al., 2012; Yildirimer et al., 2011).

When not topically applied, a necessary characteristic of silver nanoparticles is to reach the target tissue. Even if many authors demonstrated the antibacterial role of AgNPs, there are few data referring to the fate of AgNPs in the bloodstream, where they can interact with different proteins (Ban and Paul, 2016). So, it is very important for AgNPs to avoid protein adsorption on their surface that can lead to their clearance by macrophages and subsequent elimination by kidney and liver (Mandal et al., 2011; Otsuka et al., 2003). Also, the size of the carrier is important in order to avoid its clearance. It was proposed that a carrier with a diameter between 20 and 200 nm resist to the renal clearance, being maintained for an enough time in the circulation to allow the accumulation at proper concentration in the target tissue (Petrov et al., 2016).

Moreover, a good carrier should potentiate the drug effect by increasing significantly the anticancer efficiency. That will allow the use of lower doses of antitumor drug in order to suppress the developing of the drug resistance by the tumor cells (Petrov et al., 2016).

Nowadays, many efforts are made to find a proper coating agent for AgNPs, in order to increase their bioavailability and sustain their functions (Otsuka et al., 2003). Besides a long half-life period, the carrier must present a great ability to cross the endothelial wall and to enter the target tissue (Otsuka et al., 2003).

Mast cells have an important role in innate immunity, host defense and allergy, even if there is no evidence that mast cells can generate allergic processes. As we previous demonstrated mast cells are prominent in the inflammatory infiltrate of the male mice treated with topic cutaneous tumor inductors substances (Dehelean et al., 2016). Few data are available regarding the role of mast cells in the pathological processes generated after AgNPs exposure (Aldossari et al., 2015; Yang et al., 2010; Marquis et al., 2009). Even if it was stated that internalization of AgNPs by mast cells may induce their degranulation or either inhibition, the subject could be further discussed (Marquis et al., 2009; Huang et al., 2009). Alsaleh et al. appreciated that silver nanoparticles induced mast cell activation and indicated novel aspects on engineered nanoparticles and immune system activation (Alsaleh et al., 2016).

In the present study, it was demonstrated that mast cells were degranulated after media and AgNPs exposure, albeit the specimens were harvested after the first i.p. administration or at the end of the experiment. These observations contradict the results obtained by Kittler et al. who observed no degranulation after citrate or AgNPs administration, but are consistent with data published by Aldossari et al. who established a direct activation of the mast cells after AgNPs exposure (Aldossari et al., 2015; Kittler et al., 2010).

After media administration was also observed an increase in the number of mast cells. The presence of AgNPs in the solution administrated, even if stimulated the degranulation of mast cells, inhibited their number, observation consistent with data published by other authors (Kittler et al., 2010).

The administration of PEG-AgNPs had no effect on degranulation but inhibited the number of mast cells, action that was maintain for the entire period of the experiment, probably due to the capacity of PEG coat to hide AgNPs from the monocytes macrophages system and to extend their life in the blood stream. The general observation is that if these type of compounds developed such a reduced toxicity after an important route of parenteral administration they could be considered safe particles for other types of applications.

The assessment of nanoparticles impact on mast cells activity is considered a relevant toxicological test, especially when the nanomaterials will be further used for *in vivo* applications as drug delivery agents (Luo et al., 2015). The data regarding the interactions between mast cells located at skin level and silver nanoparticles administered *in vivo* as parenteral solution are rather few, and the results obtained in the present study could be considered an element of novelty. Another novel aspect discussed in this study was the reduced capacity of PEGylated citrate silver nanoparticles to induce mast cells degranulation, what might lead to an improved biological activity by avoiding the presence of the toxicity induced by the mast cells granules and immune

system activation.

5. Conclusions

Stable and non-aggregated spherical AgNPs and new PEG-AgNPs colloids could be synthesized on a single step chemical reduction by adding SDS, as capping agent. Coted silver nanoparticles – PEG-AgNPs are applicable in certain doses on biological trails and these formulations keep constant their shape in biological environment. These colloids exhibited cytotoxicity on human keratinocytes cells only at lower concentrations as an aspect of reduced toxicity. Single and multiple i.p. administration route did not induce noxious symptoms in mice appreciated by data corroborated with histological and non-invasive evaluations. At all studied time points, no significant changes were detected in terms of biochemical and hematological parameters on *in vivo* observations. New PEG-coated AgNPs at skin level determine a decreased mast cells expression and implicit a reduce immune system activation as a positive aspect. PEG-coated silver nanoparticles proved to be in acute and subacute tested interval toxicologically safe and also appropriate dosages for human use.

Conflicts of interest

The authors declare that there is no conflict of interest regarding the publication of this paper.

Acknowledgement

This work was supported by a grant of the Romanian National Authority for Scientific Research and Innovation, CNCS – UEFISCDI, project number PN-II-RU-TE-2014-4-2842.

Appendix A. Supplementary data

Supplementary data related to this article can be found at http://dx.doi.org/10.1016/j.fct.2017.11.051.

Transparency document

Transparency document related to this article can be found online at http://dx.doi.org/10.1016/j.fct.2017.11.051.

References

Ahamed, M., Alsalhi, M.S., Siddiqui, M.K., 2010. Silver nanoparticle applications and human health. Clin. Chim. Acta 411, 23–24. 1841-1848. https://doi.org/10.1016/j.cca.2010.08.016.

Alaluf, S., Atkins, D., Barrett, K., Blount, M., Carter, N., Heath, A., 2002. The impact of epidermal melanin on objective measurements of human skin colour. Pigment. Cell Res. 15 (2), 119–126.

Aldossari, A.A., Shannahan, J.H., Podila, R., Brown, J.M., 2015. Influence of physicochemical properties of silver nanoparticles on mast cell activation and degranulation. Toxicol. Vitro 29 (1), 195–203. https://doi.org/10.1016/j.tiv.2014.10.008.

Alsaleh, N.B., Persaud, I., Brown, Jared M., 2016. Silver nanoparticle-directed mast cell degranulation is mediated through calcium and PI3K signaling independent of the high affinity IgE receptor. PLoS One. https://doi.org/10.1371/journal.pone.0167366.

Arora, S., Rajwade, J.M., Paknikar, K.M., 2012. Nanotoxicology and in vitro studies: the need of the hour. Toxicol. Appl. Pharmacol. 258 (2), 151–165. https://doi.org/10.1016/j.taap.2011.11.010.

Ataei, F., 2016. Blood toxicity of silver nanoparticles in Pregnant Wistar Rats. Iran. J. Ped. Hematol. Oncol. 6 (2), 124–128.

Ban, D.K., Paul, S., 2016. Protein corona over silver nanoparticles triggers conformational change of proteins and drop in bactericidal potential of nanoparticles: polyethylene glycol capping as preventive strategy. Coll. Surf. B 146, 577–584. https://doi.org/10.1016/j.colsurfb.2016.06.050.

Banerjee, D., Sengupta, S., 2011. Nanoparticles in cancer chemotherapy. Prog. Mol. Biol. Transl. Sci. 104, 489–507. https://doi.org/10.1016/B978-0-12-416020-0.00012-7.

Bastos, V., Ferreira de Oliveira, J.M., Brown, D., Jonhston, H., Malheiro, E., Daniel-da-Silva, A.L., Duarte, I.F., Santos, C., Oliveira, H., 2016. The influence of Citrate or PEG coating on silver nanoparticle toxicity to a human keratinocyte cell line. Toxicol. Lett. 249, 29–41. https://doi.org/10.1016/j.toxlet.2016.03.005.

Benavides, F., Oberyszyn, T.M., VanBuskirk, A.M., Reeve, V.E., Kusewitt, D.F., 2009. The hairless mouse in skin research. J. Dermatol. Sci. 53 (1), 10–18. http://doi.org/10.1016/j.jdermsci.2008.08.012.

Bergin, I.L., Wilding, L.A., Morishita, M., Walacavage, K., Ault, A.P., Axson, J.L., Stark, D.I., Hashway, S.A., Capracotta, S.S., Leroueil, P.R., Maynard, A.D., Philbert, M.A., 2016. Effects of particle size and coating on toxicologic parameters, fecal elimination kinetics and tissue distribution of acutely ingested silver nanoparticles in a mouse model. Nanotoxicology 10 (3), 352–360. https://doi.org/10.3109/17435390.2015.1072588.

Code of Federal Regulations, Title 21, Volume 3, Revised as of April 1, 2017, Cite: 21CFR72.820.

Caballero-Díaz, E., Pfeiffer, C., Kastl, L., Gil, P., Simonet, B., Valcárcel, M., et al., 2013. The toxicity of silver nanoparticles depends on their uptake by cells and thus on their surface chemistry. Part. Part. Syst. Charact. 30 (12), 1079–1085. https://doi.org/10.1002/ppsc.201300215.

Chaloupka, K., Malam, Y., Seifalian, A.M., 2010. Nanosilver as a new generation of nanoproduct in biomedical applications. Trends Biotechnol. 28 (11), 580–588. https://doi.org/10.1016/j.tibtech.2010.07.006.

Chandran, P.R., Thomas, R.T., 2015. Gold nanoparticles in cancer drug delivery. In: Thomas, S., Grohens, Y., Ninan, N. (Eds.), Nanotechnology Applications for Tissue Engineering, Micro&Nanotechnologies Series. Elsevier Inc., Oxford, UK, pp. 221–237.

Ciappellano, S.G., Tedesco, E., Venturini, M., Benetti, F., 2016. In vitro toxicity assessment of oral nanocarriers. Adv. Drug Deliv. Rev. 106 (Pt B), 381–401. https://doi.org/10.1016/j.addr.2016.08.007.

Ciurlea, S., Dehelean, C.A., Cinta-Pinzaru, S., Falamas, A., Muresan, A., Loghin, F., 2012. Raman spectroscopy investigations of the CD1Nu/Nu mouse skin precarcinoma damages. Farmacia 60 (3), 448–456.

Conde, J., Doria, G., Baptista, P., 2012. Noble metal nanoparticles applications in cancer. J. Drug Deliv. 2012, 751075 12 pages. https://doi.org/10.1155/2012/751075.

Coricovac, D.E., Moacă, E.A., Pinzaru, I., Cîtu, C., Soica, C., Mihali, C.V., Păcurariu, C., Tutelyan, V.A., Tsatsakis, A., Dehelean, C.A., 2017. Biocompatible colloidal suspensions based on magnetic iron oxide nanoparticles: synthesis, characterization and toxicological profile. Front. Pharmacol. 8, 154. http://dx.doi.org/10.3389/fphar.2017.00154.

de Veik, M., Vabdenabeele, P., De Beer, T., Remon, J.P., Moens, L., 2009. Reference database of Raman spectra of pharmaceutical excipients. J. Raman Spectrosc. 40, 297–307. https://doi.org/10.1002/jrs.2125.

Dehelean, C.A., Feflea, S., Gheorgheosu, D., Ganta, S., Cimpean, A.M., Muntean, D., Mansoor, M.A., 2013. Anti-angiogenic and anti-cancer evaluation of betulin nanoemulsion in chicken chorioallantoic membrane and skin carcinoma in Balb/c mice. J. Biomed. Nanotechnol. 9 (4), 577–589.

Dehelean, C.A., Soica, C., Pinzaru, I., Coricovac, D., Danciu, C., Pavel, I., Borcan, F., Spandidos, D.A., Tsatsakis, A.M., Baderca, F., 2016. Sex differences and pathology status correlated to the toxicity of some common carcinogens in experimental skin carcinoma. Food Chem. Tox. 95, 149–158. https://doi.org/10.1016/j.fct.2016.07.007.

Djaqued, Y., Robichaud, J., Bruning, R., Albert, A.-S., Ashrit, P.V., 2005. The effect of poly (ethylene glycol) on the crystallization and phase transitions of nanocrystalline TiO_2 thin films. Mater. Sci. – Poland 23 (1), 15–27.

El-Zahry, M.R., Mahmoud, A., Refaat, I.H., Mohamed, H.A., Bohlmann, H., Lendl, B., 2015. Antibacterial effect of various shapes of silver nanoparticles monitored by SERS. Talanta 138, 183–189. https://doi.org/10.1016/j.talanta.2015.02.022.

Engin, A.B., Neagu, M., Golokhvast, K., Tsatsakis, A., 2015. Nanoparticles and endothelium: an update on the toxicological interactions. Farmacia 63 (6), 762–804.

Engin, A.E., Nikitovic, D., Neagu, M., Henrich-Noack, P., Docea, A.O., Shtilman, M.I., Golokhvast, K., Tsatsakis, A.M., 2017. Mechanistic understanding of nanoparticles' interactions with extracellular matrix: the cell and immune system. Part. Fibre Toxicol. 14, 22. https://doi.org/10.1186/s12989-017-0199-z.

Gliga, A.R., Skoglund, S., Wallinder, I.O., Fadeel, B., Karlsson, H.L., 2014. Size-dependent cytotoxicity of silver nanoparticles in human lung cells: the role of cellular uptake, agglomeration and Ag release. Part. Fibre Toxicol. 11 (1), 1. https://doi.org/10.1186/1743-8977-11-11.

Hendrickson, O.D., Klochkov, S.G., Novikova, O.V., Bravova, I.M., Shevtsova, E.F., Safenkova, I.V., Zherdev, A.V., Bachurin, S.O., Dzantiev, B.B., 2016. Toxicity of nanosilver in intragastric studies: biodistribution and metabolic effects. Toxicol. Lett. 241, 184–192. https://doi.org/10.1016/j.toxlet.2015.11.018.

Huang, Y.F., Liu, H., Xiong, X., Chen, Y., Tan, W., 2009. Nanoparticle-mediated IgE-receptor aggregation and signaling in RBL mast cells. J. Am. Chem. Soc. 131, 17328–17334.

Ivask, A., Kurvet, I., Kasemets, K., Blinova, I., Aruoja, V., Suppi, S., Kahru, A., 2014. Size-dependent toxicity of silver nanoparticles to bacteria, yeast, algae, Crustaceans and mammalian cells in vitro. PLoS One 9 (7), e102108. https://doi.org/10.1371/journal.pone.0102108.

Jiravova, J., Tomankova, K.B., Harvanova, M., Malina, L., Malohlava, J., Luhova, L., Panacek, A., Manisova, B., Kolarova, H., 2016. The effect of silver nanoparticles and silver ions on mammalian and plant cells in vitro. Food Chem. Toxicol. 96, 50–61. https://doi.org/10.1016/j.fct.2016.07.015.

Jing, X., Deng, L., Gao, B., Xiao, L., Zhang, Y., Ke, X., Lian, J., Zhao, Q., Ma, L., Yao, J., Chen, J., 2014. A novel polyethylene glycol mediated lipid nanoemulsion as drug delivery carrier for paclitaxel. Nanomed. Nanotech. Biol. Med. 10, 371–380. https://doi.org/10.1016/j.nano.2013.07.018.

Kang, H.G., Kim, S., Lee, K.H., Jin, S., Kim, S.H., Lee, K., Jeon, H., Song, Y.-G., Lee, S.-W., Seo, J., Park, S., Choi, I.-H., 2017. 5 nm silver nanoparticles amplify clinical features of atopic dermatitis in mice by activating mast cells. Small 1602363. https://doi.org/10.1002/smll.201602363.

Kittler, S., Greulich, C., Diendorf, J., Köller, M., Epple, M., 2010. Toxicity of silver

nanoparticles increases during storage because of slow dissolution under release of silver ions. Chem. Mater. 22, 4548–4554. https://doi.org/10.1021/cm100023p.
Koenig, J.L., Angood, A.C., 2003. Raman spectra of poly (ethylene glycols) in solution. J. Polym. Sci. Part A-2 8, 1787–1796. https://doi.org/10.1002/pol.1970.160081013.
Kuskov, A.N., Shtilman, M.I., Villemson, A.L., Larionova, N.I., Tsatsakis, A.M., Tsikalas, I., Rizos, A.K., 2007. Amphiphilic poly-N-vinylpyrrolidone nanocarriers with incorporated model proteins. J. Phys. Condens. Matter 19 (20), 5139–5150. https://doi.org/10.1088/0953-8984/19/20/205139.
Kuskov, A.N., Kulikov, P.P., Goryachaya, A.V., Tzatzarakis, M.N., Docea, A.O., Velonia, K., Shtilman, M.I., Tsatsakis, A.M., 2017. Amphiphilic poly-N-vinylpyrrolidone nanoparticles as carriers for non-steroidal, anti-inflammatory drugs: in vitro cytotoxicity and in vivo acute toxicity study. Nanomed. NBM 13 (3), 1021–1030. https://doi.org/10.1016/j.nano.2016.11.006.
Lankveld, D.P., Oomen, A.G., Krystek, P., Neigh, A., Troost-de Jong, A., Noorlander, C.W., Van Eijkeren, J.C., Geertsma, R.E., De Jong, W.H., 2010. The kinetics of the tissue distribution of silver nanoparticles of different sizes. Biomaterials 31 (32), 8350–8361. https://doi.org/10.1016/j.biomaterials.2010.07.045.
Lansdown, A.B.G., 2010. A pharmacological and toxicological profile of silver as an antimicrobial agent in medical devices. Adv. Pharmacol. Sci 16 pages. https://doi.org/10.1155/2010/910686.
Larsen, S.T., Nielsen, G.D., Thygesen, P., 2002. Investigation of the adjuvant effect of polyethylene glycol (PEG) 400 in BALB/c mice. Int. J. Pharm. 231, 51–55.
Liu, D., Yu, S., Zhu, Z., Lyu, C., Chunping Bai, C., Huiqi Ge, H., Yang, X., Pan, W., 2014. Controlled delivery of carvedilol nanosuspension from osmotic pump capsule: in vitro and in vivo evaluation. Int. J. Pharm. 475, 496–503. https://doi.org/10.1016/j.ijpharm.2014.09.008.
Luo, Y.H., Chang, L.W., Lin, P., 2015. Metal-based nanoparticles and the immune system: activation, inflammation, and potential applications. Biomed. Res. Int. 1–12. https://doi.org/10.1155/2015/143720.
Man, M.-Q., Lin, T.-K., Santiago, J.L., Celli, A., Zhong, L., Huang, Z.-M., et al., 2014. Basis for enhanced barrier function of pigmented skin. J. Invest. Dermatol. 134 (9), 2399–2407. http://doi.org/10.1038/jid.2014.187.
Mandal, A., Meda, V., Zhang, W.J., Farhan, K.M., Gnanamani, A., 2011. Synthesis, characterization and comparison of antimicrobial activity of PEG/TritonX-100 capped silver nanoparticles on collagen scaffold. Coll. Surf. B 90, 191–196. https://doi.org/10.1016/j.colsurfb.2011.10.021.
Maryamabadi, A., Hasaninejad, A., Nowrouzi, N., Mohebbi, G., Asghari, B., 2016. Application of PEG-400 as a green biodegradable polymeric medium for the catalyst-free synthesis of spiro-dihydropyridines and their use as acetyl and butyrylcholinesterase inhibitors. Bioorg. Med. Chem. 24, 1408–1417. https://doi.org/10.1016/j.bmc.2016.02.019.
Marquis, B.J., Maurer-Jones, M.A., Braun, K.L., Haynes, C.L., 2009. Amperometric assessment of functional changes in nanoparticle-exposed immune cells: varying Au nanoparticle exposure time and concentration. Analyst 134, 2293–2300.
McShan, D., Ray, P.C., Yu, H., 2014. Molecular toxicity mechanism of nanosilver. J. Food Drug Anal. 22 (1), 116–127. https://doi.org/10.1016/j.jfda.2014.01.010.
Mendis, P., de Silva, R.M., de Silva, K.M.N., Wijenayaka, L.A., Jayawardana, K., Yan, M., 2016. Nanosilver Rainbow: a rapid and facile method to tune different colours of nanosilver through the controlled synthesis of stable spherical silver nanoparticles. RSC Adv. 6, 48792–48799. https://doi.org/10.1039/C6RA08336F.
Mohanta, Y.K., Panda, S.K., Bastia, A.K., Mohanta, T.K., 2017. Biosynthesis of silver nanoparticles from protium serratum and investigation of their potential impacts on food safety and control. Front. Microbiol. 8, 626. https://doi.org/10.3389/fmicb.2017.00626.
Muhamad, I.I., Selvakumaran, S., Lazim, N.A.M., 2014. Designing polymeric nanoparticles for targeted drug delivery system. In: Seifalian, A., de Mel, A., Kalaskar, D.M. (Eds.), Nanomedicine. One Central Press (OCP), Manchester, UK, pp. 287–313.
Muhammad, Z., Raza, A., Ghafoor, S., Naeem, A., Naz, S.S., Riaz, S., Ahmed, W., Rana, N.F., 2016. PEG capped methotrexate silver nanoparticles for efficient anticancer activity and biocompatibility. Eur. J. Pharm. Sci. 91, 251–255. https://doi.org/10.1016/j.ejps.2016.04.029.
Najafi-Hajivara, S., Zakeri-Milanic, P., Mohammadid, H., Niazia, M., Soleymani-Goloujeha, M., Baradarand, B., Valizadeh, H., 2016. Overview on experimental models of interactions between nanoparticles and the immune system. Biomed. Pharmacother. 83, 1365–1378. https://doi.org/10.1016/j.biopha.2016.08.060.
Neagu, M., Piperigkou, Z., Karamanou, K., Engin, A.B., Docea, A.O., Constantin, C., et al., 2017. Protein bio-corona: critical issue in immune nanotoxicology. Arch. Toxicol. 91 (3), 1031–1048. https://doi.org/10.1007/s00204-016-1797-5.
Nguyen, K.C., Richards, L., Massarsky, A., Moon, T.W., Tayabali, A.F., 2016. Toxicological evaluation of representative silver nanoparticles in macrophages and epithelial cells. Toxicol. Vitro 33, 163–173. https://doi.org/10.1016/j.tiv.2016.03.004.
Otsuka, H., Nagasaki, Y., Kataoka, K., 2003. PEGylated nanoparticles for biological and pharmaceutical applications. Adv. Drug Deliv. Rev. 55 (3), 403–419.
Pang, C., Brunelli, A., Zhu, C., Hristozov, D., Liu, Y., Semenzin, E., Wang, W., Tao, W., Liang, J., Marcomini, A., Chen, C., Zhao, B., 2016. Demonstrating approaches to chemically modify the surface of Ag nanoparticles in order to influence their cytotoxicity and biodistribution after single dose acute intravenous administration. Nanotoxicology 1–11. Early Online. https://doi.org/10.3109/17435390.2015.1024295.
Pacioni, N.L., Borsarelli, C.D., Rey, V., Veglia, A.V., 2015. Synthetic routes for the preparation of silver nanoparticles. A mechanistic perspective. In: Alarcon, E.I. (Ed.), Silver Nanoparticle Applications, Engineering Materials, . https://doi.org/10.1007/978-3-319-11262-6_2.
Petrov, P.D., Yoncheva, K., Gancheva, V., Konstantinov, S., Trzebicka, B., 2016. Multifunctional block copolymer nanocarriers for co-delivery of silver nanoparticles and curcumin: synthesis and enhanced efficacy against tumor cells. Eur. Polym. J. 81, 24–33. https://doi.org/10.1016/j.eurpolymj.2016.05.010.
Phongtongpasuk, S., Poadang, S., Niti Yongvanich, N., 2016. Environmental-friendly method for synthesis of silver nanoparticles from dragon fruit peel extract and their antibacterial activities. Energy Procedia 89, 239–247. https://doi.org/10.1016/j.egypro.2016.05.031.
Piperigkou, Z., Karamanou, K., Engin, A.B., Gialeli, C., Docea, A.O., Vynios, D.H., Pavão, M.S.G., Golokhvast, K.S., Shtilman, M.I., Argiris, A., Shishatskaya, E., Tsatsakis, A.M., 2016. Emerging aspects of nanotoxicology in health and disease: from agriculture and food sector to cancer therapeutics. Food Chem. Tox. 91, 42–57. https://doi.org/10.1016/j.fct.2016.03.003.
Pulit-Prociak, J., Stoklosa, K., Banach, M., 2015. Nanosilver products and toxicity. Environ. Chem. Lett. 13, 59–68. https://doi.org/10.1007/s10311-014-0490-2.
Ragaseema, V.M., Unnikrishnan, S., Krishnan, K.V., Krishnan, L.K., 2012. The antithrombotic and antimicrobial properties of PEG-protected silver nanoparticle coated surfaces. Biomaterials 33 (11), 3083–3092. https://doi.org/10.1016/j.biomaterials.2012.01.005.
Riaz Ahmed, K.B., Nagy, A.M., Brown, R.P., Zhang, Q., Malghan, S.G., Goering, P.L., 2017. Silver nanoparticles: significance of physicochemical properties and assay interference on the interpretation of in vitro cytotoxicity studies. Toxicol. Vitro 38, 179–192. https://doi.org/10.1016/j.tiv.2016.10.012.
Saifuddin, N., Wong, C.W., Nur Yasumira, A.A., 2009. Rapid biosynthesis of silver nanoparticles using culture supernatant of bacteria with microwave irradiation. E-J. Chem. 6 (1), 61–70. https://doi.org/10.1155/2009/734264.
Sharma, V.K., Siskova, K.M., Zboril, R., Gardea-Torresdey, J.L., 2014. Organic-coated silver nanoparticles in biological and environmental conditions: fate, stability and toxicity. Adv. Colloid Interface Sci. 204, 15–34. https://doi.org/10.1016/j.cis.2013.12.002.
Soica, C., Oprean, C., Borcan, F., Danciu, C., Trandafirescu, C., Coricovac, D., Crăiniceanu, Z., Dehelean, C.A., Munteanu, M., 2014. The synergistic biologic activity of oleanolic and ursolic acids in complex with hydroxypropyl-γ-cyclodextrin. Molecules 19 (4), 4924–4940. https://doi.org/10.3390/molecules19044924.
Soica, C., Coricovac, D., Dehelean, C., Pinzaru, I., Mioc, M., Danciu, C., Fulias, A., Puiu, M., Sitaru, C., 2016. Nanocarriers as tools in delivering active compounds for immune system related pathologies. Recent Pat. Nanotechnol. 10 (2), 128–145.
Taylor, S., Westerhof, W., Im, S., Lim, J., 2006. Noninvasive techniques for the evaluation of skin color. J. Am. Acad. Dermatol. 54 (5), S282–S290. https://doi.org/10.1016/j.jaad.2005.12.041.
Tejamaya, M., Romer, I., Merrifield, R.C., Lead, J.R., 2014. Stability of citrate, PVP, and PEG coated silver nanoparticles in ecotoxicology media. Environ. Sci. Technol. 46 (13), 7011–7017. https://doi.org/10.1021/es2038596.
Turkevich, J., Stevenson, P.C., Hillier, J., 1951. A study of the nucleation and growth processes in the synthesis of colloidal gold. Discuss. Faraday Soc. 11, 55–75. https://doi.org/10.1039/DF9511100055.
Turner, P.V., Brabb, T., Pekow, C., Vasbinder, M.A., 2011. Administration of substances to laboratory animals: routes of administration and factors to consider. J. Am. Assoc. Lab. Anim. Sci. 50 (5), 600–613.
Varner, K.E., el-Badawy, A., Feldhake, D., Venkatapathy, R., 2010. State-of the- Science Review: Everything Nanosilver and More. EPA/600/R-10/084. U.S. Environmental Protection Agency, Washington, DC.
Wei, L., Lu, J., Xu, H., Patel, A., Chen, Z.S., Chen, G., 2015. Silver nanoparticles: synthesis, properties, and therapeutic applications. Drug Discov. Today 20 (5), 595–601. https://doi.org/10.1016/j.drudis.2014.11.014.
Williams, K.M., Gokulan, K., Cerniglia, C.E., Khare, S., 2016. Size and dose dependent effects of silver nanoparticle exposure on intestinal permeability in an in vitro model of the human gut epithelium. J. Nanobiotechnol. 14, 62. http://dx.doi.org/10.1186/s12951-016-0214-9.
Yamini, D., Venkatasubbu, G.D., Kumar, J., Ramakrishnan, V., 2014. Raman scattering studies on PEG functionalized hydroxyapatite nanoparticles. Spectrochim. Acta Part A Mol. Biomol. Spectrosc. 117, 299–303. https://doi.org/10.1016/j.saa.2013.07.064.
Yang, W., Lee, S., Lee, J., Bae, Y., Kim, D., 2010. Silver nanoparticle-induced degranulation observed with quantitative phase microscopy. J. Biomed. Opt. 15, 045005.
Yildirimer, L., Thanh, N.T.K., Loizidou, M., Seifalian, A.M., 2011. Toxicological considerations of clinically applicable nanoparticles. Nano Today 6, 585–607.
Zook, J.M., Halter, M.D., Cleveland, D., Long, S.E., 2012. Disentangling the effects of polymer coatings on silver nanoparticle agglomeration, dissolution, and toxicity to determine mechanisms of nanotoxicity. J. Nanopart. Res. 14, 1165. https://doi.org/10.1007/s11051-012-1165-1.